People's Democratic Republic of Algeria
Ministry of Higher Education and Scientific Research

Amar Thelidji University – Laghouat

FACULTY: TECHNOLOGY

DEPARTMENT: PROCESS ENGINEERING

MASTER THESIS

Presented by: BENARFA Mohamed Tayeb

HAYANI Riyad

DOMAIN: Science and Technology

SECTOR: Process Engineering.

OPTION: Chemical Engineering

Theme

INSIGHT INTO THE PHYSICAL PROPERTIES OF THE COMPOUND Ag_2BaSnS_4: DFT STUDY

Jury de soutenance :

First and last name	Grade	Quality
BOUTASSOUNA Nassima	MAA	President
Hannachi Manelle	MCB	Examiner
BELHADJ Soraya	MCB	Advisor
/	/	Co-rapporteur (if applicable)

Academic year: 2024

Dedications

Praise be to God, we praise Him and thank Him, who has guide us to value my academic journey with this memorandum, the result of seventeen years of seriousness and diligence. As for what follows:

I dedicate this humble work to those who have all the credit for bringing me to this moment after God Almighty My precious and precious treasure, may God protect them and prolong their lives, my mother and father.

To my support in this world after my generous parents, the source of joy and happiness, my brothers and sisters: Zakaria, Djaafar, Ikram, Inas.

Of course, I will not forget Allal Benarfa, who was credited with following this academic path.

To my partner in this work, the kind colleague Hayani Riyad, to my loved ones, my friends, my classmates, to everyone who helped me, even if just a letter, each in his name, each in his position.

My sincere thanks and gratitude to you. May you stay safe and in good health and may God protect you all.

BENARFA Mohamed Tayeb

Dedications

This thesis is dedicated to my beloved family. To my parents, whose love and sacrifices have been my greatest motivation.

To my siblings, who have always been my biggest cheerleaders. Your support and belief in me have been the driving force behind this achievment.

HAYANI Riyad

Acknowledgments

We would like to first of all thank Allah the Almighty Who guided and helped us to accomplish this modest work.

Our thanks also go to our supervising Dr. BELHADJ Soraya who spent her time supervising this scientific research and provided us with all the informations and advices we needed, so this modest work came to an end and came into being.

We are also so honored to have Dr. HANNACHI Manelle and Dr. BOUTASSOUNA Nassima as members in the jury of this work.

And since this work was accomplished within the physics and chemistry of materials laboratory of AMAR THELIDJI University of LAGHOUAT we would not like to miss the opportunity to thank the head of the laboratory.

And also, we do not forget to thank the head of GC Dr. BELARBI Faiza and the head of process engineering department Mr. BENALIA Mokhtar.

We extend our sincere thanks to all the honorable professors of the process engineering department and to all our colleagues, process engineering students, each in their own name and position and to all the two honorable families, especially our dear parents, may God give them and our friends a long life.

List of abbreviations

APW: augmented plane wave

DFT: density functional theory

DOS: density of states

FP-LAPW: linearused augmented plane wave method

GGA: generalized gradient approximation

LDA: local density approximation

LSDA: local spin density approximation

TB-mBJ: Tran-Blaha modified Beck-Johnson

E_H: hartree energy

EOS: equation of state

H: hamiltonien

$\boldsymbol{\varepsilon_r}$**:** dielctric function (real part)

$\boldsymbol{\varepsilon_i}$**:** dielctric function (imaginary part)

List of tables

List of Figures

Content

Content

Chapter II: Results and discussion

General introduction

General introduction

Since the creation of man in previous eras, science and technology are constantly evolving. We cannot separate one science from another or separate one discipline from another, since sciences are interconnected links that form the chain of the universe, for example, we cannot study a chemical reaction by absence of the laws of physics or the logic of mathematics.

Condensed matter physics and materials science are fundamentally concerned with understanding and exploiting the properties of systems of interacting electrons and atomic nuclei. This has been well known since the development of quantum mechanics. Unfortunately, the electrons and nuclei that make up materials constitute a strongly interacting and this makes solving the Schrödinger equation extremely difficult, and as stated by Dirac; progress depends on the development of sufficiently precise approximate techniques. Thus the development of density functional theory (DFT) [1] with the local density approximation (LDA) [2] and the generalized gradient approximation (GGA) [3] played an important role in condensed matter physics. These techniques for calculating physicochemical properties are which have now become a basic tool for calculating the structural, electronic and optical properties of the most complex systems. These techniques are based on simulations; that replaced the experiment, sometimes expensive, inaccessible to the laboratory. The basic formalism of DFT is based on the Hohenberg-Kohn theorem [4]. This approach applies to any system with several interacting particles evolving in an external potential, implemented in the wien2k simulation code.

Our objective is to study the properties of compound A with the wien2k code. So, our work consists of the following parts:

- General introduction.
- CHAPTER I: Bibliographic review.
- CHAPTER II: Calculations, results and discussion.
- General conclusion.

References

[1]: P. Hohenberg, W. Kohn. Inhomogeneous electron gas. *Physical Review* 136(3B) (1964) B864-B871.

[2]: D.M. Ceperley, B.J. Alder. Ground state of the electron gas by a stochastic method. *Physical Review Letters* 45(7) (1980) 566-569.

[3]: J.P. Perdew, Y. Wang. (1992). Accurate and simple analytic representation of the electron-gas correlation energy. *Physical Review B* 45(23) (1992) 13244-13249.

[4]: W. Kohn, L.J. Sham. (1965). Self-consistent equations including exchange and correlation effects. *Physical Review* 140(4A) (1965) A1133-A1138.

Chapter I:

Bibliographic review

I.1. Introduction

Man has experienced a wide range of physical systems: metals, insulators, superconductors or even semiconductors. All of these materials have greatly improved the quality of our lives. For years, without a doubt, semiconductors have revolutionized the world of physics thanks to their exceptional properties [1].

I.2. Materials concepts

I.2.1. Materials choosing

Materials are at the source of technology and industrial world. The technical and commercial successes of a manufactured product depend largely on the material(s) chosen. Selecting a material is generally not a simple operation given the wide variety of available families. In the context of product design, the main goal of material selection is to minimize cost while meeting sample performance goals. Systematic selection of the best material for a given application begins with properties and costs of candidate materials. Selection is often benefited by the use of material index or performance index relevant to the desired properties. For example, a superconductor must have a zero electrical resistance inside, this is why an electric current can circulate forever in a superconducting ring even when the battery has been unplugged this is how magnetic fields are created [2].

I.2.2. Types of materials

A material is of natural or artificial origin that men use and/or design to manufacture objects, construct buildings or machines.

Materials are differentiated according to their origin (from living beings for example) and their properties, whether mechanical (flexibility or rigidity, etc.), chemical (permeability or impermeability to water, etc.) or even physical (conductivity of the electricity or heat, etc.). They are generally classified into different large families:

- **Metallic materials** which include:
    - Metals: iron, copper, bronze, etc.
    - Metal alloys: stainless steel, etc.
- **Organic materials** that come from living beings, plants or animals (wood, cotton, paper, etc.).

- **Mineral or inorganic materials**: rock, ceramic, glass, etc.
- **Composite materials** which combine several materials from different families to obtain multiple properties (carbon fiber, etc.) [3].

Figure I.1: Main families of materials.

I.2.3. Materials properties

I.2.3.1. Physical properties

Pure metals most often have high electrical conductivity, thermal conductivity and density. Silver is thus the best electrical conductor (6.30×10^7 S/m), followed by copper (5.96×10^7 S/m), gold (4.10×10^7 S/m) and aluminum (3.50×10^7 S/m).The electrical conductivity of iron is 10^7 S/m, while that of 1010 carbon steel (0.10% carbon iron) is only 5.9×10^6 S/m, illustrating the effect of impurities on the conductivity of metals [4].

Although most metals have a density greater than that of most non-metals, this varies greatly depending on the materials considered. Among simple metallic bodies, lithium is the least dense (0.534 $g.cm^{-3}$ at 25 °C) while osmium is the densest (22.59 $g.cm^{-3}$). Alkaline metals (which include lithium) and alkaline earth metals are the least dense of the metals; they are also the least hard, and the alkali metals have a particularly low melting point: apart from lithium, they are all liquid at 100 °C. The high density of most metals comes from their compact crystal structure [5].

Metals are also generally characterized by good malleability and high ductility which allow them to deform without breaking. Thus, pure copper can be stretched to form electrical wires, pipes (plumbing), be plated and hammered into the shape of pans; Pure gold can also be formed into very thin sheets. Conversely, certain alloy elements make it possible to harden the metal: this is for example the case of carbon which hardens iron to give steel, tin which hardens copper to give family, at the refractory metals, because these elements have a large number of delocalized electrons in their structure. However,

other factors also come into play, such as the atomic radius, the atomic number, the number of bonding orbitals, the superposition of the energies of the orbitals and the type of crystal structure; Centered cubic structures thus give weaker metallic bonds than face-centered cubic and compact hexagonal structures because the latter have a higher coordination, that is to say they bind more neighboring atoms than the first.

I.2.3.2. Mechanical properties

Hooke's law can model the elastic deformation of metals when the deformation is a linear function of the stress. The application of forces greater than the elastic limit or heating can lead to permanent deformation of the object, which corresponds to plastic deformation [6]. This irreversible modification of the arrangement of the atoms of the material can result from the application:

- A force or work in tension , compression, shearing, bending or torsion.
- Heating, which affects the mobility of structural defects in the material, such as grain boundaries, vacancies, screw and corner dislocations, and stacking faults of crystalline and non-crystalline solids. The movement of such defects requires activation energy and is therefore limited by the atomic diffusion rate.

Viscous flow around grain boundaries, for example, can give rise to creep or metal fatigue. It can also contribute to significant changes in microstructure, such as grain growth and localized increase in material density by elimination of intergranular porosity. Additionally, the non-directional nature of metal bonds could contribute significantly to the ductility of solid metals [7].

I.3. Classification

I.3.1. Classification of chemical elements

The atoms of chemical elements differ by their structure at the subatomic scale, that is to say the number and nature of the elementary particles, which constitute them:

- **Nucleus:** protons and possibly neutrons.
- **Electronic procession gravitating around the nucleus**: electrons in numbers equal to the protons in an atom in equilibrium [8].

The protons are positively charged and the electrons negatively, have equal elementary charges in absolute values, so that the atom is electrically neutral in the equilibrium

state (figure I.2). The mass of the electron is negligible compared to that of the proton or neutron (table I.1).

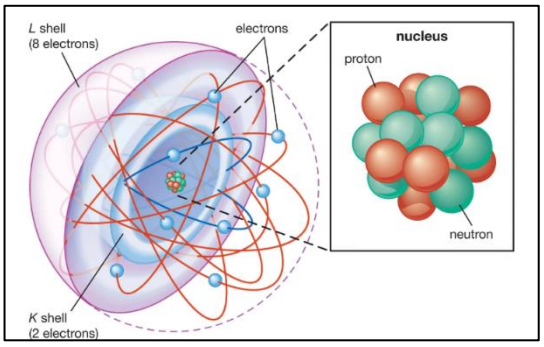

Figure I.2: Simplified representation of an atom.

The orbits of electrons occupy successive layers in an atom, corresponding to discrete energy levels, which become bands in solids grouping several atoms. These levels can only contain a limited number of electrons: two for the first, eight for the following levels (at least when they are in the external position), and forbidden bands separate them. We call the Fermi energy of the atom considered the upper limit of the filling of the electronic energy states at thermodynamic equilibrium and at absolute zero [9].

Table I.1: Mass and electric charges of elementary particles.

	Mass (kg)	Mass (amu)	Charge (relative)	Charge (C)
Proton	1.67262×10^{-27}	1.00727	+I	$+1.60218\times10^{-19}$
Neutron	1.67493×10^{-27}	1.00866	0	0
Electron	0.00091×10^{-27}	0.00055	-I	$-1.60218\times^{-19}$

In the periodic classification table of chemical elements; Mendeleev table (table I.2 and I.3); the lines or periods are the successive levels of the electronic layers. The columns or groups are the number of electrons in the outer layer.

From the second element of the fourth period (calcium), the internal electronic layers can receive more than eight electrons so additional elements are intercalated before moving to the next group. The chemical properties of an element come essentially from its electrons, and in particular those in the outer layer, called valence electrons, these properties are therefore linked to the group (column of the periodic table) to which it belongs.

Isotopes: Elements with the same atomic number (and therefore the same electronic and chemical properties), but different atomic masses, due to a different number of

neutrons. In nature, some chemical elements exist as mixtures of isotopes; this results in non-integer average atomic mass values.

Group properties: Elements of group VIII, called rare gases, are characterized by a complete outer layer which gives them exceptional chemical stability.

The elements of group I A (table I.2) have only one electron in their outer layers: they tend to get rid of it to have a saturated outer layer and give positive ions or cations.

Table I.2: Periodic classification of chemical elements principle.

	Group I	**Group II**	**Group III**	**Group IV**	**Group V**	**Group VI**	**Group VII**	**Group VIII**
1st period (K-band)	Z=1 A=1  Hydrogen H							Z=2 A=4  Helium He
2nd period (bands k and l)	Z=3 A=7  Lithium Li	Z=4 A=9  Beryllium Be	Z=5 A=11  Boron B	Z=6 A=12  Carbon C	Z=7 A=14  Nitrogen N	Z=8 A=16  Oxygen O	Z=9 A=19  Fluor F	Z=10 A=20  Neon Ne
3rd period (bands k and l and m)	Z=11 A=23  Sodium Na	Z=12 A=24  Magnesium Mg	Z=13 A=27  Aluminum Al	Z=14 A=28  Silicon Si	Z=15 A=31  Phosphorus P	Z=16 A=32  Sulfur S	Z=17 A=35  Chlorine Cl	Z=18 A=40  Argon Ar

Table I.3: Periodic classification of elements.

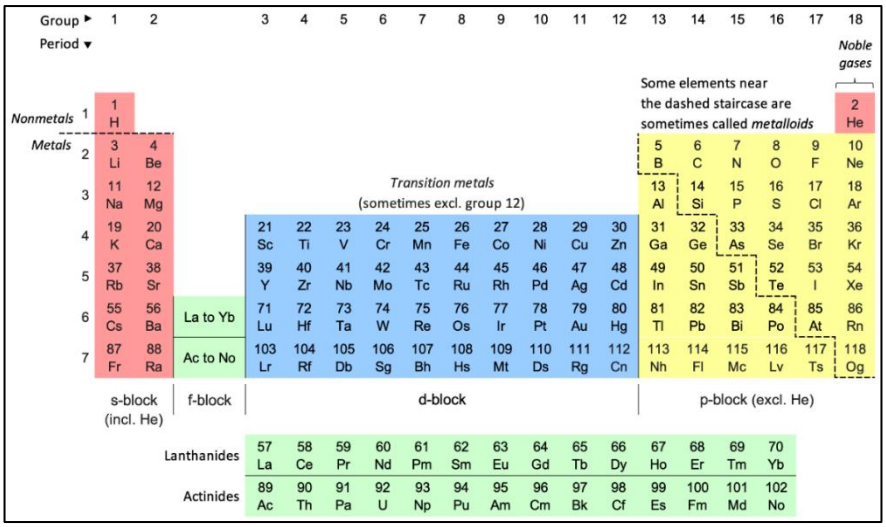

This trend also extends to all the elements on the left side of the table, called metals, which are all electron donors. Group VII A elements have seven electrons in their outer shells: they tend to complete it by capturing an available electron in their neighborhood to give negative ions or anions.

This trend also extends to certain elements on the right side of the table, called non-metals, they all electron acceptors. Certain elements located at the boundary between these two zones have mixed characteristics, varying depending on the electric field to which they are subjected (they are semiconductors). Figure I.3 illustrates these differences in behavior by the band structures of these various types of atoms.

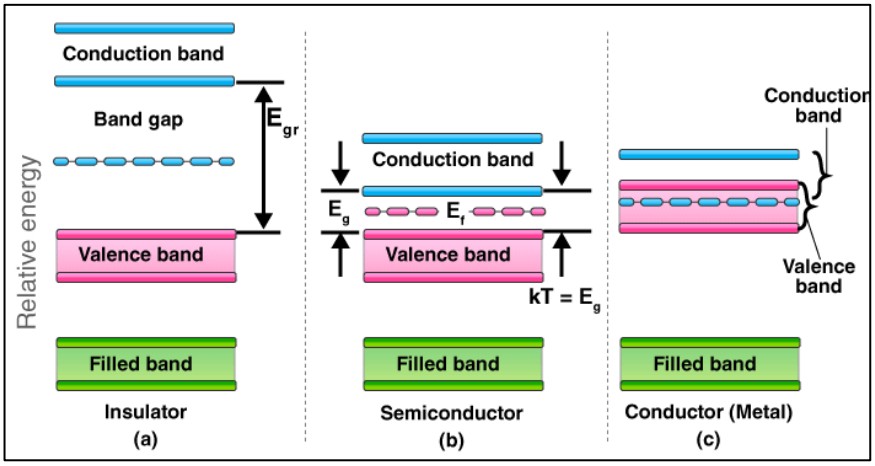

Figure I.3: Diagrams of band structures.

- Non-metal atoms (insulator), the band gap has a large ΔE width.
- Semiconductor atoms, the band gap has a small ΔE width.
- Metal atoms, the conduction band has available states.

I.3.2. Classification of materials and properties

I.3.2.1. Main classes of materials

Many physicochemical properties and usage properties of materials are closely linked to the nature of the chemical bonds between the atoms that constitute them. on this basis that the distinction between the main classes of materials is established.

Metal materials: These are pure metals and their mixtures, or alloys, essentially comprising metallic bonds [10].

Organic materials: These are materials of biological origin, synthetic polymers and elastomers, comprising covalent bonds and weak bonds [11].

Mineral materials: These are rocks, oxides, mineral glasses, ceramics containing ionic bonds and/or covalent bonds [12].

Composite materials: They combine different materials in a structured, fine-scale manner, possibly belonging to different classes among the three previous ones [13].

I.3.2.2. Usage properties

The physicochemical properties and usage properties of materials are multiple and can be subject to various classifications. Some are mainly conditioned by the nature of the atoms and chemical bonds present mainly in the material: density, mechanical and thermal stability, melting temperature, elastic flexibility or rigidity, fragility or ductility, electrical and thermal conductivity, magnetic properties, etc.

Some are sensitive to the structure according to which the atoms are arranged and organized: plastic rigidity, hardness, ductility, tenacity, etc.

I.3.2.3. Principle properties of main materials classes

a. Metal materials

Metallic materials are considered have different property values according to the property itself. This is well established in figure I.4.

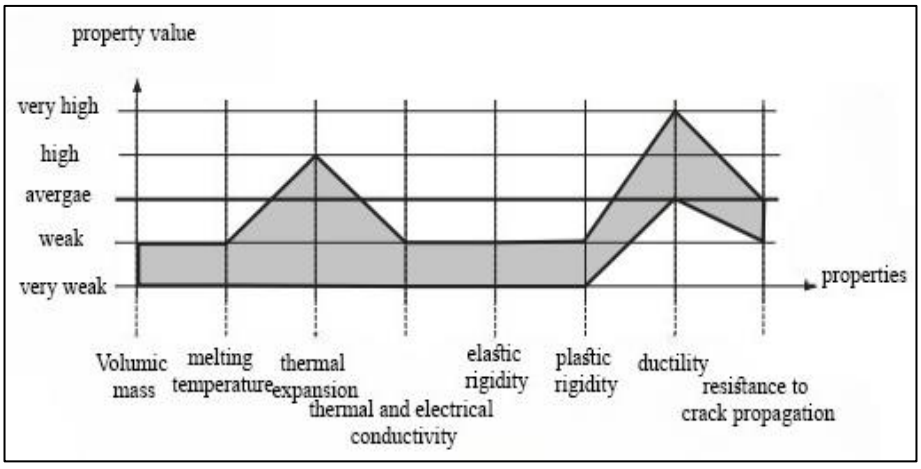

Figure I.4: Comparing the property value of metal materials based on their property.

b. Organic materials

Relation between property value and property for organic material is represented in figure I.5.

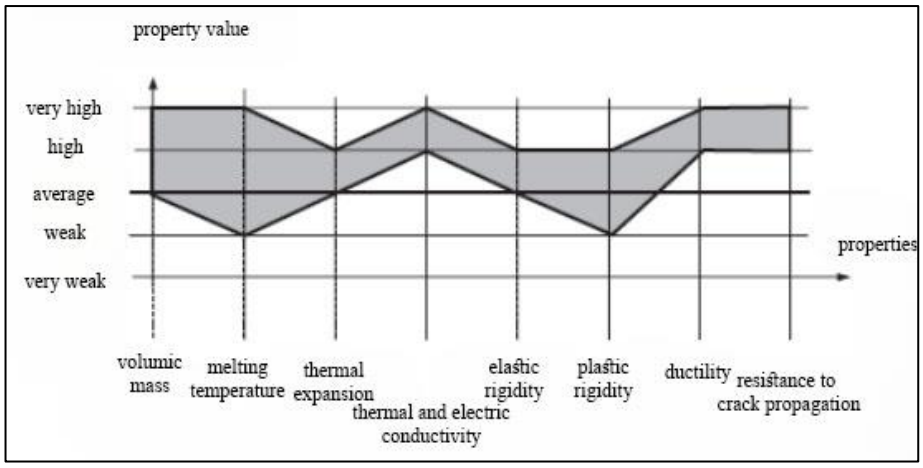

Figure I.5: Comparing the property value of organic materials based on their property.

c. Mineral materials

For mineral materials, figure I.6 illustrates the property value-property relationship.

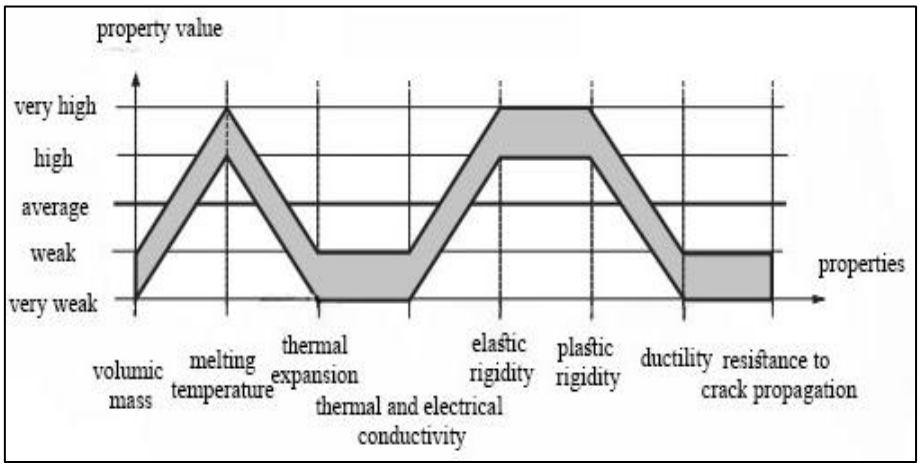

Figure I.6: Comparing the property value of mineral materials based on their property.

d. Composite materials

Depending on their structure and the nature of their components, the properties of composite materials are extremely variable: for the most part, they are intermediate between the properties of the materials that constitute them. Sometimes, however, certain emergent properties (properties resulting from the entire structure and constituents of the material) can take on unexpected values.

I.4. Crystalline solids

A crystal is a set of atoms (or molecules) arranged periodically in three directions and exhibiting both short-range and long-range order. It can be defined from two data: crystal structure and the atomic pattern.

I.4.1 Crystal structure

It is a three-dimensional set of imaginary points, the nodes, arranged periodically in the three directions of space. It can be generated by repetition, an integer number of times, of three basis vectors which define an elementary cell of the arbitrary original network. Therefore, the nodes of the network are all the points of the integer coordinate space in the chosen basis (figure I.4). The nodes are arranged in rows and reticular planes.

There are seven main primitive crystal structures and fourteen lattices named Bravais systems. In table I.4 are regrouped their corresponding characteristics.

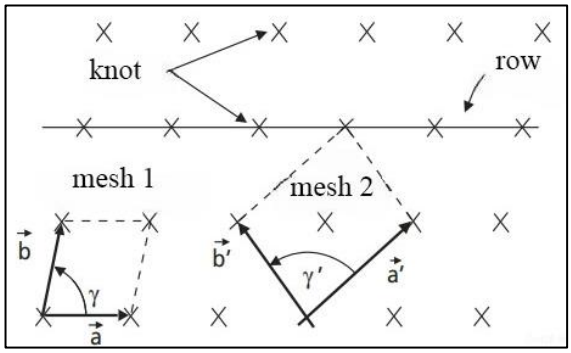

Figure I.7: Diagram of a two-dimensional network: Mesh No. 1 is an example of an elementary mesh (one knot per mesh). Mesh N° 2 is an example of a multiple mesh.

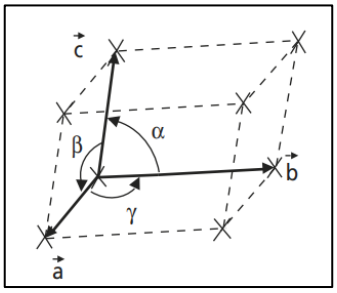

Figure I.8: Mesh construction.

An infinite number of possibilities exist for the choice of the elementary cell and its three basic vectors (lengths a, b, c, angles α, β, γ). For the sake of simplicity, the choice generally falls on the mesh presenting the maximum number of symmetry elements (planes and axes of symmetry), which sometimes leads to choosing a multiple mesh (mesh containing several nodes of the network). Topological considerations relating to the tiling of three-dimensional space by periodic repetition of identical volumes without void or overlap, lead to the conclusion that there can only exist seven different types of meshes, defining the seven primitive crystal systems (figure I.7).

Table I.4: Definition of the crystallographic reference frame and characteristics of the meshes of the seven primitive crystal systems and the fourteen Bravais lattices.

Primitive crystal system	Bravais networks	Vector lengths	Vector angles	Example
Triclinic	Simple	$\vec{a} \neq \vec{b} \neq \vec{c}$	$\vec{\alpha} \neq \vec{\beta} \neq \vec{\gamma} \neq \frac{\pi}{2}$	
Monoclinic	Simple, with centered bases	$\vec{a} \neq \vec{b} \neq \vec{c}$	$\vec{\alpha} = \vec{\beta} = \frac{\pi}{2} \neq \vec{\gamma}$	
Orthorhombic	Simple, centered, with centered bases, with centered faces	$\vec{a} \neq \vec{b} \neq \vec{c}$	$\vec{\alpha} = \vec{\beta} = \vec{\gamma} = \frac{\pi}{2}$	U_{α}, Fe_3C
Quadratic	Simple, centered	$\vec{a} = \vec{b} \neq \vec{c}$	$\vec{\alpha} = \vec{\beta} = \vec{\gamma} = \frac{\pi}{2}$	Martensite
Hexagonal	Simple	$\vec{a} = \vec{b} \neq \vec{c}$	$\vec{\alpha} = \vec{\beta} = \frac{\pi}{2} = \vec{\gamma} = 2\pi/3$	Zn, Mg
Rhombohedral	Simple	$\vec{a} = \vec{b} = \vec{c}$	$\vec{\alpha} = \vec{\beta} = \vec{\gamma} \neq \frac{\pi}{2}$	As, Sb, Bi
Cubic	Simple, centered, face-centered	$\vec{a} = \vec{b} = \vec{c}$	$\vec{\alpha} = \vec{\beta} = \vec{\gamma} = \frac{\pi}{2}$	Fe, Cu, Al

In some of these primitive meshes, additional nodes can be added to the center of the mesh, to the centers of two bases or to the centers of the six faces without losing the properties of periodicity and symmetry of the corresponding networks. We obtain fourteen Bravais networks [14].

I.5. Conductivity

Solid materials are classified according to their conductivities into three types: conductive materials, insulating materials and semiconductor materials.

We have adapted this classification on the basis of a band structure of the material and on a band gap (energy interval) GAP which separates between the valence band and the conduction band [15].

In an insulator, the value of the gap is so large that the electrons cannot pass from the valence band to the conduction band: the electrons do not circulate in the solid. In semiconductors this value is smaller and zero in the conductor. The valence band is rich in electrons but does not participate in conduction phenomena (for electrons). The conduction band, for its part, is empty of electrons. However (metals), the conduction band and the valence band overlap. The electrons can therefore pass directly from the valence band to the conduction band and circulate throughout the solid.

In a semiconductor, as in an insulator, these two bands are separated by a band gap, commonly called by (GAP).

The only difference between a semiconductor and an insulator is the width of this band gap, a width which gives each its respective properties.

The following figure represents E_{Gap} in the three material classes.

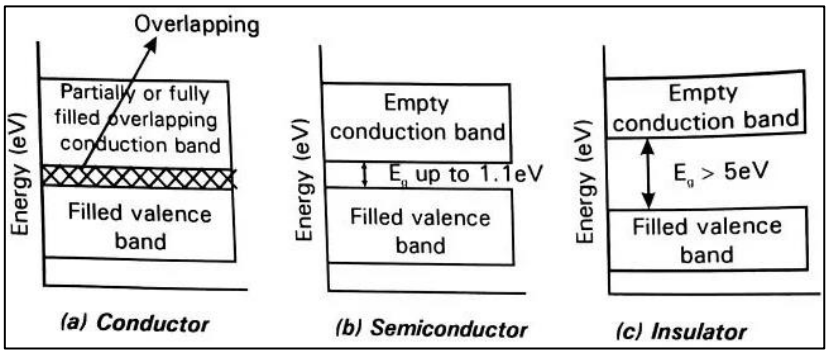

Figure I.9: Theoretical diagram established according to the theory of energy bands indicating, depending on the case, the respective position of the valence band and the conduction band.

I.5.1. Semiconductors

A semiconductor, like silicon, is a material that is neither quite a conductor of electricity nor quite an insulator. It can be either one or the other depending on various conditions. The conductive or insulating nature takes its source from the structure of atoms: each element of the periodic table has a certain number of electrons which are arranged around a nucleus. It is this arrangement in the form of layers of electrons, different depending on the elements, which is responsible for electrical conductivity.

The electrons of an atom can have several roles within an atom structure:

- **Core electrons:** these are close to the nucleus and do not really interact with other atoms.
- **Valence electrons:** these are on the outer layers of the atom and make it possible to create interatomic bonds and form molecules.
- **Conduction electrons:** these are responsible for the circulation of electric current.

We see that in a metal, some electrons are in both the valence band and the conduction band. This means that a metal can conduct current without any other form of physico-chemical treatment. In an insulator, on the other hand, the two bands are separated by a space called the "gap band": this means that electrons cannot be found there. In the case of insulators, the external electrons are all in the valence band and none are in the conduction band: these materials cannot conduct electricity. In the case of

semiconductors, in the middle, there is also a band gap, but it is very thin. All it takes is a little something for the valence electrons to pass into the conduction band and this make the semiconductor... conductive. We manage to do this by giving energy to the electrons, by exciting them [16].

I.5.2. Direct gap, indirect gap

I.5.2.1. Direct bandgap

In direct bandgap semiconductor, the bottom of the conduction band and top of the valence band lies at the same value of K. In this, electron can directly excite or de-excite by the absorption or emission of photon and there is no phonon involvement in the process of excitation and de-excitation.

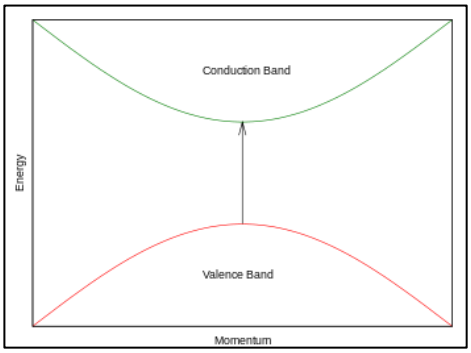

Figure I.10: Direct bandgap.

I.5.2.2. Indirect bandgap

in Indirect bandgap semiconductor, top of the valence band and bottom of the conduction band lies at different values of K. If an electron goes from the top of the valence band to the bottom of the conduction band, it has to change its energy as well as wave-vector K [17].

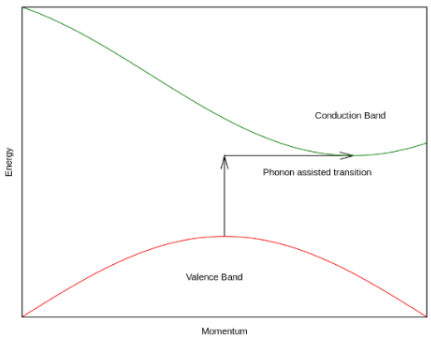

Figure I.11: Indirect bandgap.

I.5.3. Chemical bonds

There are different chemical bonds depending on the electronic cloud form and their energy levels. In solids there are two types of bond:

I.5.3.1. Strong bonds

- **Covalent bond:** the sharing of two electrons to complete the outer shell of each atom ensures it. It appears between two non-metal atoms (bond provided by electrons from the valence band).
- **Ionic bond:** the transfer of an electron from one atom to another ensures it. It appears between an atom of a metal and an atom of a non-metal. After bonding, the two atoms become electrically charged ions.
- **Metallic bond:** The sharing of electrons from the peripheral layer ensures it; the "gas" constituted by these free and delocalized electrons ensures the cohesion of all the remaining cations. It appears between the elements of a cluster of metal atoms (bond provided by the electrons of the conduction band). The electrons in the metallic bond are mobile and available to ensure the possible circulation of an electric current.

I.5.3.2. Weak bonds

These are simple electrostatic attractions between electric charges of opposite signs. They appear between the + and – poles of molecules with inhomogeneous or polarizable charge distributions. They act at a longer distance, but with a lower intensity than strong bonds.

I.6. Density functional theory DFT

Density Functional Theory or DFT forms today one of the most used methods in quantum calculations of the electronic structure of matter (atoms, molecules, solids) both in physics of condensed matter than in quantum chemistry. DFT finds its origins in the model developed by Llewellyn Thomas and Enrico Fermi at the end of the 1920s. However, it was not until the mid-1960s and the contributions of Pierre Hohenberg, Walter Kohn and Lu Sham that the theoretical formalism was established. on which the current method is based. Methods respecting traditions in theories of the electronic structure of matter, especially the Hartree-Fock theory and methods derived from this formalism, are based on a multielectron wave function. The main goal of density

functional theory is to replace the multielectron wave function with electron density as the basic quantity for calculations. While the multielectron wave function depends on 3N variables (where N is the total number of particles in the device), the density is only a function of three variables; it is therefore an easier quantity to treat both mathematically and conceptually. The principle of DFT consists of a reformulation of the N-body quantum problem into a one-body problem (or, strictly speaking, two-body if we consider spin problems) with the electron density as a parameter. The central idea of DFT is that the unique electron density of the essential state of the device entirely determines the average values of observables such as energy.

DFT theory was originally primarily developed within the framework of non-relativistic quantum theory (time-independent Schrödinger equation) and the Born–Oppenheimer approximation. The theory was then extended to the domain of time-dependent quantum mechanics (we then speak of TDDFT for Time-Dependent Density Functional Theory) and to the relativistic domain. DFT is also used for the thermodynamic description of classical fluids [18].

I.6.1 Schrödinger equation

The geometric structure, vibration modes as well as other observables describe the electronic structure of the system studied with «N electrons» and «M nuclei». Classical mechanics remains insufficient and we must resort to quantum mechanics, the basis of which is the resolution of the Schrödinger equation. This electronic structure is deduced from the time-independent multi-electron Schrödinger equation:

$$H.E = \psi.E \quad \text{.....I.1}$$

With: H: The Hamiltonian operator.

Ψ: The wave function of the system.

E: Clean energy.

I.6.2. Hohenberg and Kohn theorems

The development of density functional theory began in 1964 and 1965 with the publications of Hohenberg and Kohn (1964). The two theorems are as follows:

Theorem 01: The total energy of the fundamental state E is a unique functional of the particle density $\rho(\vec{r})$ for an external potential $V_{ext}(\vec{r})$ given. This theorem means that it is enough to know only the electron density to determine all the wave functions.

Consequently, the total energy E of a system of interacting electrons in an external potential is represented as a functional of the electron density of the fundamental state,ρ_0[19].

Theorem 02: The total energy functional of any multi-particle system has a minimum which corresponds to the fundamental state. The particle density of the fundamental state verifies:

$$E[\rho_0] = \min E(\rho) \quad \text{.....I.2}$$

Hohenberg and Kohn showed that the true density of the fundamental state is that which minimizes the energy $[\rho_0]$, and all other properties are also a functional of this density. The energy of the fundamental state of an electronic system in an external potential is determined by the variational method [20].

I.6.3. Kohn Sham theorem

In 1965 Kohn and Sham (KS) proposed a practical method for using density functional theory. These authors considered the equivalence between a system of electrons interacting in an external potential V and a system of electrons without interaction in an effective potential V_{eff} therefore, the functional of energy [21].

I.6.4. Exchange potential and LDA and GGA correlation

In principle DFT gives us a good description of fundamental state properties, these practical applications are based on approximations for the correlation exchange potential which describes the effects of the Pauli principle and the Coulomb potential beyond a pure electrostatic interaction between electrons.

Exact knowledge of the correlation exchange potential means that we have solved the multi-body problem exactly. Among the most used approximations currently is the local density approximation (LDA) which locally substitutes the energy density □_xc of exchange correlation of a non-homogeneous system with that of a gas, of electrons of the same density.

I.6.4.1. Local Density Approximation (LDA)

The local density approximation (LDA) consists of treating an inhomogeneous system, as locally homogeneous (uniform gas of interacting electrons where ρ is constant). Consequently, the Energy of exchange and correlation depends only on the electron

density at a point r, neglecting any influence of the inhomogeneity of the system (or considers that the density varies very slowly). It is expressed according to the Energy of exchange and correlation per particle [22].

I.6.4.2. Generalized Gradient Approximation (GGA)

Generalized gradient approximation was introduced to improve the accuracy of LDA results. It consists of writing the exchange and correlation Energy not only as a function of the electron density but also of its gradient to take into account the non-uniform nature of the electron gas. This approximation is divided into (03) approximations:

- WC-GGA.
- PBE-GGA.
- PBE-SOL-GGA.

I.6.4.3. Approximation WC-GGA

The major gap in the two approximations (GGA and LDA) is the estimation of the value of the energy gap, which is essentially due to the correlation term which is considered too simple, and to correct this gap, Engel and Vosko showed that the GGA does not improve on the second order expansion of the generalized gradient due most of the time to the cancellation of local errors hence the correction made to the correlation term, we mix the second order of the generalized gradient with the exact Hartree-Fock correlation term. This new form called: (EVGGA) turns out to be better for the calculation of the gap, but unfortunately it remains poor if we are interested in the calculations of the fundamental Energy according to the structural parameters [23].

I.6.4.4. Approximation PBE-SOL

Popular modern generalized gradient approximations are biased when describing free atom energies. Restoring the first-principles gradient for exchange over a wide range of density gradients eliminates this bias.

Perdew et al introduced a generalized Perdew-Burke-Emzerof gradient approximation that improves the equilibrium properties of densely packed solids and their surfaces.

I.6.4.5. Approximation of TB-mBJ

In this sense, other improvements have been made such as the TB-mBJ approximation proposed by Tran and Blaha in 2009. The Tran and Blaha functional noted (mBJ) is a modified version of the Becke and Johnson functional. The latter quickly proved its

effectiveness compared to the most often used calculation methods such as LDA and GGA [24]. Messrs. Tran and Blaha propose in their article published on June 3, 2009 in physical review letters, a modified version of the Becke and Johnson functional, in the form:

$$v_{x,\sigma}^{MBJ}(r) = cv_{x,\sigma}^{BR} + (3c-2)\frac{1}{\pi}\sqrt{\frac{5}{12}}\sqrt{\frac{2t_\sigma(r)}{\rho_\sigma}} \quad \text{..... I.3}$$

with:

$\rho_\sigma = \sum_{i=1}^{N_\sigma} \left|\psi_{i,\sigma}\right|^2$ Electron density.

$t_\sigma(r) = \frac{1}{2}\sum_{i=1}^{N_\sigma} \left|\psi_{i,\sigma}^{*}\nabla_{\psi_{i},\sigma}\right|^2$ Kinetic energy density.

$v_{X,\sigma}^{MBJ}(r)$ The potential of Becke-Roussel.

I.7. Wien2k calculation code

The WIEN2k package is a computer program written in Fortran which performs quantum mechanical calculations on periodic solids. It uses the full-potential (linearized) augmented plane-wave and local-orbitals [FP-LAPW+lo] basis set to solve the Kohn–Sham equations of density functional theory.

Peter Blaha and Karlheinz Schwarz from the Institute of Materials Chemistry of the Vienna University of Technology originally developed WIEN2k. The first public release of the code was done in 1990 [25].

Then, the next releases were WIEN93, WIEN97, and WIEN2k.The latest version WIEN2k_23.2 was released in February 2023. It has been licensed by more than 3400 user groups and has about 16000 citations on Google scholar (Blaha WIEN2k).

Figure I.12: Wien2k code logo.

I.7.1. The main steps to follow in the WIEN2K code

When using this code, we generally go through three steps.

I.7.1.1. Initialization

This step is done for the preparation of the SCF cycle. During this step, a series of subprograms are executed, among which we cite:

N: is a program that lists the distances between nearest neighbors, which helps determine the value of the atomic radius of the sphere (R_{MT}).

SGROUP: it determines the space group of the structure that is defined in the case (CIF) file.

SYMMETRY: is a subprogram which lists the symmetry operations of the space group of our structure from the information contained in the case file (CIF).

LSTART: A program that generates atomic densities and determines how different orbitals are treated in calculating band structure, such as core states with or without local orbitals.

KGEN: this subprogram generates a mesh of points K in the irreducible part of the first Brillouin zone (IBZ). We specify the number of points K in the entire first Brillouin zone.

DSTART: this subroutine subprogram produces a first crystal charge density (case.clmsum), an initial density for the SCF (self-consistent field) by superposition of atomic densities.

I.7.1.2. SCF calculation

The initialization part allowed the creation of all the inputs for the SCF cycle, the process is then launched and iterates until the solution converges. This cycle is made up of five sub-programs:

LAPW0: is a sub-program which calculates the total potential as the sum of the Coulomb potential VC and the exchange and correlation potential V_{XC}.

LAPW1: is a sub-program that finds the Hamiltonian, overlap matrix, eigenvalues and eigenvectors by a diagonalization method.

LAPW2: is a sub-program that calculates valence electron densities from eigenvectors, it uses **case.energy** et **case.vector** and calculates E_F (Fermi level).

LCORE: is a sub-program that calculates core states and densities.

MIXER: is a sub-program that mixes the valence and core densities to produce a new density that will be used in the next iteration.

I.7.1.3. Exploring material properties

After the SCF calculation, we have all the data, in particular the Total Energy at equilibrium and the structural parameters, which allow us to examine the properties of the materials we wish to study.

After having summarized the main steps seen in the progress or execution of the WIEN2K code, we recall in the following part the main files that are necessary to execute certain programs or the files generated as output.

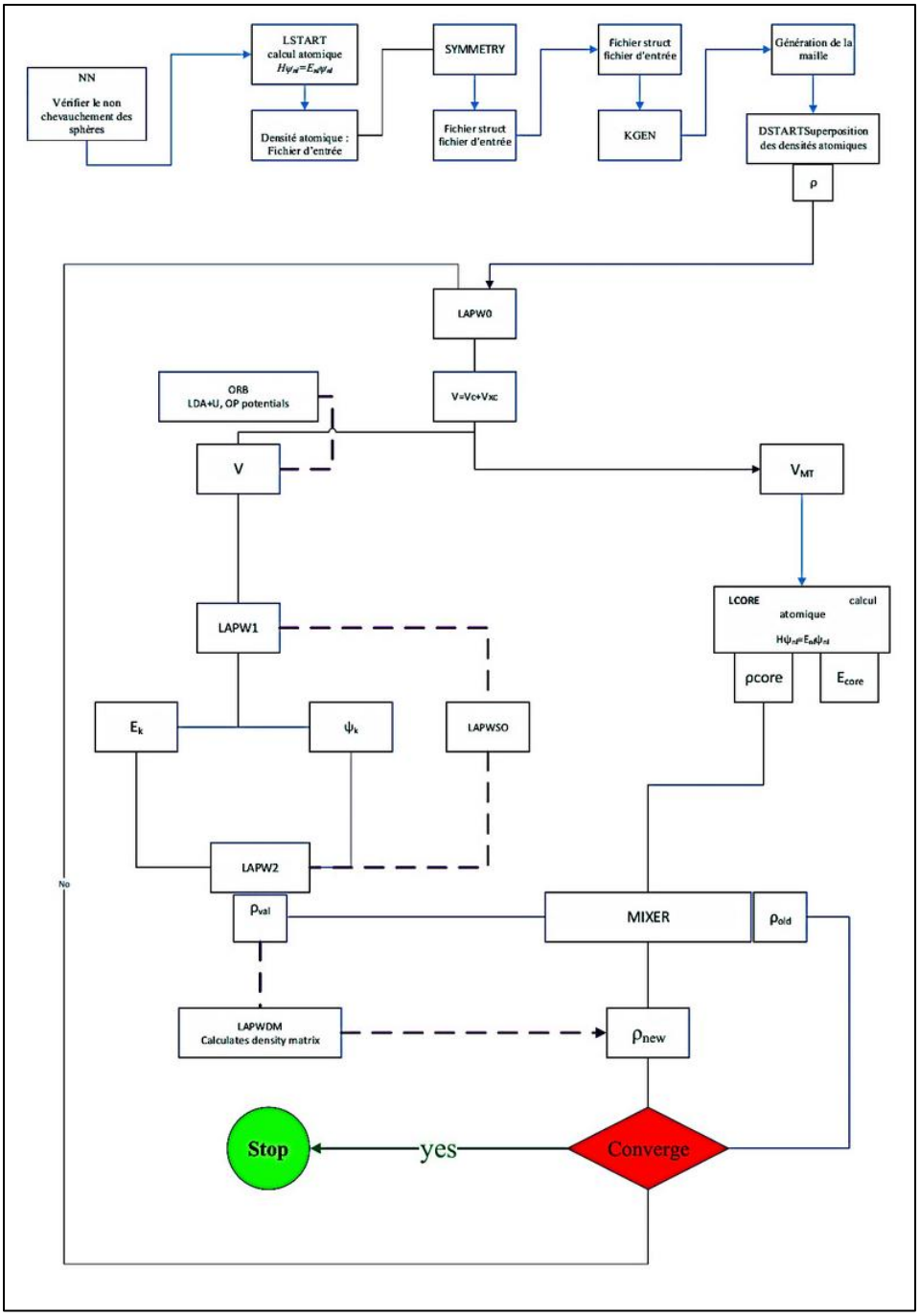

Figure I.13: Wien2k code structure.

I.8. Origin 2019

Origin is a proprietary computer program for interactive scientific graphing and data analysis. It is produced by OriginLab Corporation, and runs on Microsoft Windows. It

has inspired several platform-independent open-source clones and alternatives like LabPlot and SciDAVis.

Graphing support in Origin includes various 2D/3D plot types.

Figure I.14: Origin ver.19 logo.

Data analyses in Origin include statistics, signal processing, curve fitting and peak analysis. Origin's curve fitting is performed by a nonlinear least squares fitter which is based on the Levenberg-Marquardt algorithm.

Origin imports data files in various formats such as ASCII text, Excel, NI TDM, DIADem, NetCDF, SPC, etc. It also exports the graph to various image file formats such as JPEG, GIF, EPS, TIFF, etc. There is also a built-in query tool for accessing database data via ADO.

I.9. Conclusion

In this chapter We have generally studied materials, we can say that density functional theory is a very effective tool for the study of interacting electron systems. Indeed, it reduces the problem with N interacting bodies to that of N independent bodies which move in an effective potential.

References

[1]: M.A. Williams. *Semiconductor materials for high-speed optoelectronics.*

[2]: G.E. Dieter. *Overview of the materials selection process* (1997).

[3]: *Chemical physics*. Retrieved from CEA: https://www.cea.fr/comprendre/Pages/physique-chimie/essentiel-sur-materiaux.aspx

[4]: W.F. Smith. *Principles of materials science and engineering* (1990).

[5]: *MatWeb, Your Source for Materials Information*. Retrieved from MatWeb: https://matweb.com/

[6]: M.H. Sadd. *Elasticity: theory, applications, and numerics.*

[7]: Retrieved from https://clarolineconnect.univ-lyon1.fr/: https://clarolineconnect.univ-lyon1.fr/clarolinepdfplayerbundle/pdf/3112949

[8]: *Atome*. Retrieved from wikipedia: https://fr.wikipedia.org/wiki/Atome#

[9]: M. Dupeux. *Science et génie des matériaux* (2018).

[10]: *Metal.* Retrieved from wikipedia: https://fr.wikipedia.org/wiki/M%C3%A9tal#cite_ref-1

[11]: *Organic matter*. Retrieved from wikipedia: https://en.wikipedia.org/wiki/Organic_matter

[12]: *Minéral.* Retrieved from wikipedia: https://fr.wikipedia.org/wiki/Min%C3%A9ral

[13]: *Composite material*. Retrieved from wikipedia: https://en.wikipedia.org/wiki/Composite_material

[14]: J. Hook, H. Hall. *Solid State Physics* (2010).

[15]: *Band gap*. Retrieved from wikipedia: https://en.wikipedia.org/wiki/Band_gap#References

[16]: *Semiconductors*. Retrieved from byjus: https://byjus.com/jee/semiconductors/

[17]: *Direct and indirect band gaps*. Retrieved from wikipedia: https://en.wikipedia.org/wiki/Direct_and_indirect_band_gaps

[18]: Density functional theory and application to atoms and molecules. *Physics Reports* (2014) 123-239.

[19]: J. Stephen, C.C. Klippenstein. *Density functional theory*. In A.C. Dimian. *Computer Aided Chemical Engineering* (1997).

[20]: C.C.M. Rindt, S.G.-N. Hohenberg–Kohn theorems. In L.F. Cabeza. *Advances in Thermal Energy Storage Systems* (2015).

[21]: W.K. Sham. Self-consistent equations including exchange and correlation effects. *Physical Review* A1133 to A1138.

[22]: *Local-density approximation*. Retrieved from wikipedia: https://en.wikipedia.org/wiki/Local-density_approximation

[23]: V. Valentin, S.B. Karasiev. Advances in quantum chemistry. In *Advances in Quantum Chemistry* (2015) 221-245.

[24]: D. Reyes-coronado, G. Rodríguez-gattorno, M.E. Espinosapesqueira, *et al.* Phase-pure TiO_2 nanoparticles: anatase, brookite and rutile. Nanotechnology 19(14) (2008) 145605.

[25]: P. Blaha, K. Schwarz, P. Sorantin, S.B. Trickey. *Comput. Phys. Commun.* 59 (1990) 399.

Chapter II:

Calculations, results, and discussion

II.1. Introduction

The materials considered in this study was investigated with regard to its structural, electronic, and optical properties via Ab Initio calculations using the calculation code WIEN2K [1]. The materials studied is the quaternary chalcogenide Ag_2BaSnS_4; also called selenide.

II.2. Calculation details and parameters

II.2.1. Methods adopted

The calculation launch for each material with WIEN2K is started by the manual introduction of an input density generated by the following data:

- Atomic number Z of each element in the material considered.
- Crystal system (Bravais lattice and space group).
- Cell parameters (a, b, c, α β and γ).
- Positions of atoms (x, y, z).

II.2.1.1. Code WIEN2K

Calculations made with WIEN2k have the following details:

- Method: FP-LAPW; all electron (full potential-linearized augmented plane waves) [2]
- Approximation: WC-GGA (Wu and Cohn Generalized Gradient Approximation) [3].
- Exchange-correlation potential: TB-mBJ (Tran and Blaha modified Becke-Johnson potential) [4].
- Calculated properties: structural, electronic (band structure, total and partial density of states, and charge density) and linear optical (dielectric function ω, absorption coefficient I, reflictivity R, energy loss L, and index of refraction n).
- Theory: DFPT (density functional pertubation theory) [5].

II.2.2. Convergence step

Before any calculation of properties, convergence studies followed by optimization must be carried out. In the convergence stage, the most important criteria are the relative

variations of the total energy as a function of the calculation parameters: RK_{max} and ngkpt parameters.

It should be noted that the choice of the R_{MT} rays (muffin-tin rays) of the atoms (table II.1) is made to reduce the interstitial space as much as possible, because this region is treated by plane waves, which makes the calculation time more important.

The values adopted for the calculation parameters are cross-referenced in (table II.2). For the $R_{MT}K_{max}$ parameter it is taken equal to 7 (default values between 6 and 8).

Table II.1: Valence state and Muffin-Tin rays **R_{MT}** of Ag_2BaSnS_4constituent elements.

Element	Valence state	R_{MT} (Bohr)
Ag	$4p^6 5s^1 4d^{10}$	2.44
Ba	$4d^{10} 5p^6 6s^2$	2.5
Sn	$5s^2 4d^{10} 5p^2$	2.34
S	$3s^2 3p^4$	1.92

Table II.2: The **k-points** grid (points of sampling of Irreducible Brillouin Zone IBZ).

Compound	Grid (ngkpt)
Ag_2BaSnS_4	10x10x10 [a]
	12x12x12 [b]

[a] for the calculation of structural and electronic properties.

[b] for calculating optical properties.

II.2.3. Optimization step

The optimization step serves to relax the structure. An optimized structure corresponds to a minimum total energy, with atoms relaxed in a balanced environment translated by minimal resultant forces and Hellmann-Feynman forces (exerted on the atoms) canceled. The optimization is done using the BFGS program [6]. Often, several cycles are necessary to obtain a well-optimized structure.

It should be noted that optimization with WIEN2K serves to relax the structure.

II.3. Study of the compound Ag_2BaSnS_4

We have invested the compounds Ag_2BaS_4Sn with regard to the calculation of its properties by the code WIEN2K.

Our objective is to invest the above-mentioned properties by the introduction of the potential TB-mBJ (Becke-Johnson potential modified by Tran and Blaha) in order to obtain more adequate values of the forbidden band (gap energies) [7]. The TB-mBJ

potential turns out to be more precise in estimating the gap for materials containing metals in their structure.

In each step of the calculations (detailed below), our results were compared on one hand with experimental results, and on another hand with theoretical results (if existing).

II.3.1. Structural properties of Ag_2BaSnS_4

Ag_2BaSnS_4 crystallizes in the space group I222 (No. 23) of the orthorhombic class (figure II.1), with a = 6.8540Å, b = 7.122 Å, c = 8.136 Å, and Z = 2 (number of molecules in a unit cell). The corresponding numerical values are reported in tables II.3 and II.4.

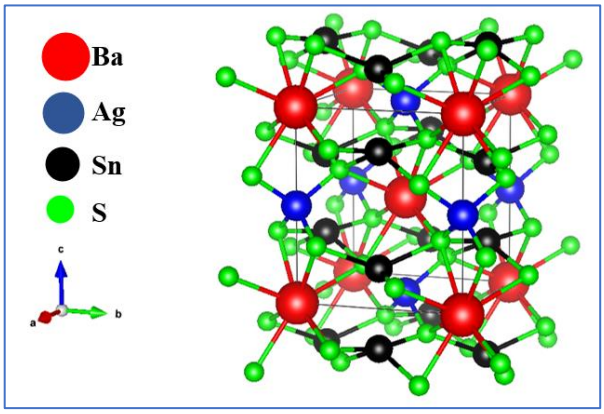

Figure II.1: (a) Orthorhombic primitive cell of Ag_2BaSnS_4*.

*Drawn from CIF file by VESTA software [8].

Table II.3: Ag_2BaS_4Sn structural parameters.

a (Å)	b (Å)	c (Å)	α/β/γ (°)	V(Å³)/Z	Space group/N°	Crystal class	Ref.
6.885	7.122	8.136	90/90/90	399/2	I222/23	Orthorhombic	[9]

Table II.4: Atomic coordinates for Ag_2BaSnS_4.

Atom	x	y	z
Ba	0	0	0
Ag	0	0.5	0.2052
Sn	0	0	0.5
S	0.2980	0.3064	0.8320

The quaternary non-centrosymmetric (NCS) sulfide, Ag_2BaS_4Sn, was synthesized from a high-temperature solid-state reaction using $BaCl_2$ flux in evacuated closed silica tubes. In its structure, highly distorted AgS_4 tetrahedra interconnect together *via* corner-sharing to form two-dimensional (2D) layers (figure II.2.a), which are further bridged with isolated SnS_4 units to produce a three-dimensional (3D) framework structure with Ba cations lying

in the tunnels (figure II.2.b). Additional structural details are shown in figure II.3. Remarkably, it not only possesses phase-matchable (PM) ability but also exhibits a good balance between strong SHG response (0.4×$AgGaS_2$) and high LIDT (1.5×$AgGaS_2$) [9].

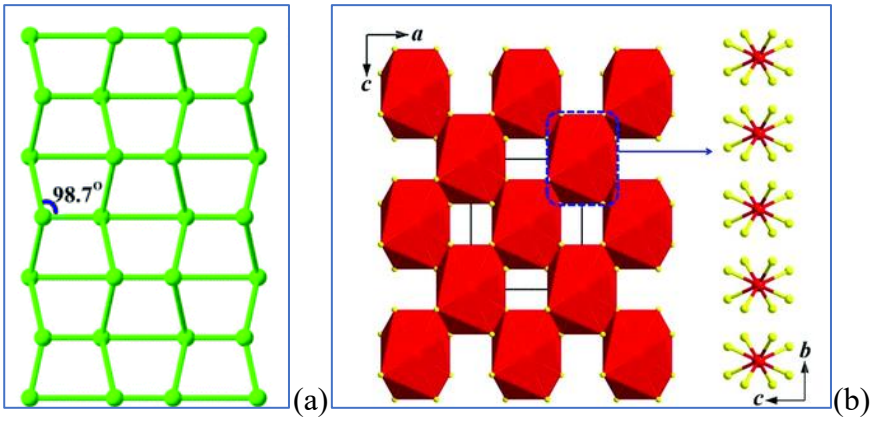

Figure II.2: (a) 2D wave-like Ag-S layer (the S atoms are omitted for a better view). (b) BaS_8 polyhedra *via* corner- and edge-sharing to make up the 3D framework structure in the *ac* plane with the unit cell marked (left), isolated BaS_8 polyhedra locate in the same tunnel (blue dashed-box) alone the *a*-axis (right) [9].

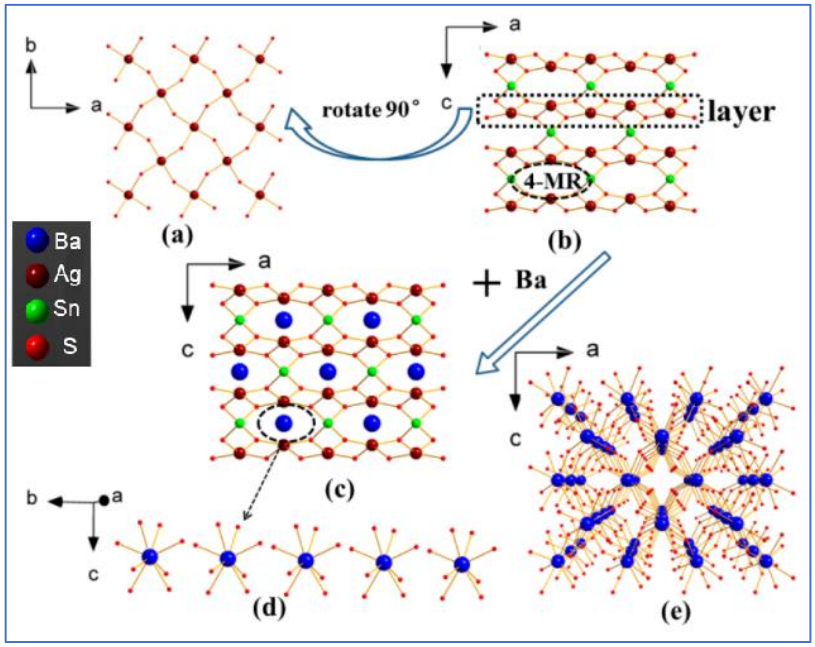

Figure II.3: Detailed structure of Ag_2BaSnS_4 [10] (with some modifications).

(a) The two-dimensional (2D) $[AgS_4]_\infty$ layer in Ag_2BaSnS_4.
(b) The 2D $[AgS_4]_\infty$ layers are bridged with $[SnS_4]$ ligands to make up 4-membered ring (MR) tunnel.
(c) The Ba cations located inside the 4-MR tunnels.
(d) The $[BaS_8]$ polyhedra are isolated in the same tunnel.
(e) Adjacent $[BaS_8]$ polyhedra interconnect by corner sharing to form 3D framework.

II.4. Structural properties

The cell parameters a, b, and c and the atomic positions are calculated and the results are analyzed.

The following general positions are assigned to the constituent elements [9]:

- Ag (0; ;z).
- Ba (⅓;⅔;z).
- Sn (0;1;z).
- S (0;0;0).

Then, optimization of volume, c/a ratio, and b/a ratio were carried out and the results are presented in figure II.4. The numerical results are reported in table II.5.

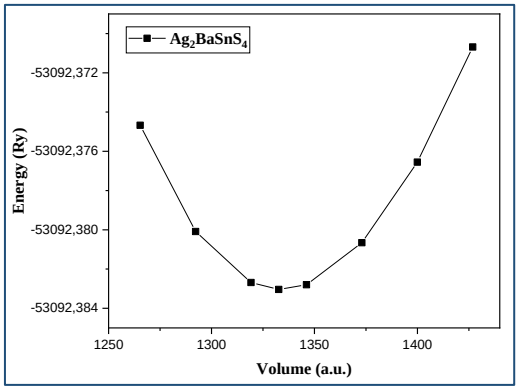

(a)

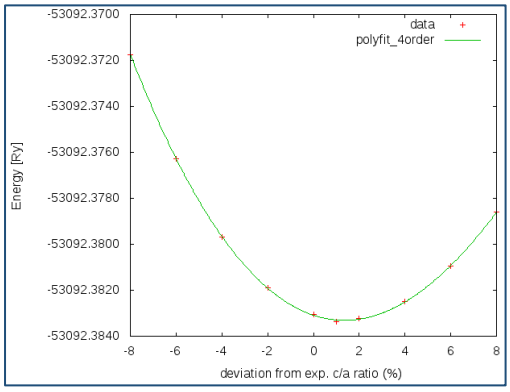

(b)

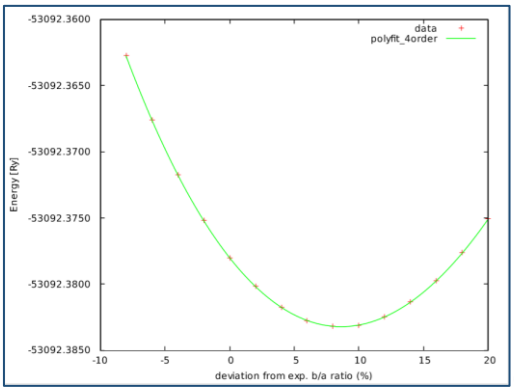

(c)

Figure II.4: Structural parameters optimization: (a); volume optimization, (b); c/a ratio optimization, (c); b/a ratio optimization.

Table II.5: Simulated and experimental structural parameters of Ag_2BaSnS_4.

Ag_2BaSnS_4	Experimental	This work (WC-GGA)	Deviation (%)
a (Å)	6.885	6.854	-0.4516
b (Å)	7.122	7.044	-1.0887
c (Å)	8.136	8.180	+0.544
V(Å^3)	399	394.96	-1.0125

From the results reported in table II.4, we note that the values of a, b, and c are estimated with acceptable deviations varying between 1.08% and 0.45% in absolute values. These results are consistent with the general trend of the GGA (FP-LAPW) approximation, which usually overestimates the structural parameters [11] (note here that the a and c-parameters have conversely been underestimated). Consequently, the volume is underestimated with tolerable discrepancy of 1.01%.

At this point, we deem it necessary to discuss the lengths of bonds by comparing the experimental values with those obtained with the optimized structures.

In fact, we report the following figures:

- For Ba-S bonds: 3.292-3.336 Å [9] versus 3.274-3.339 Å calculated: deviation of -0.55 and +0.90%.
- For Ag-S bonds: 2.786 Å [9] versus 2.766 Å calculated: deviation of -0.72%.
- For Sn-S bonds: 2.388 Å [9] versus 2.380 Å calculated: deviation of -0.33%.

The calculated bond lengths are very close to the experimental values with deviations ranging between 0.99% and 0.33% and are considered acceptable deviations.

II.5. Electronic properties

The electronic structures of Ag_2BaSnS_4 have been calculated and the following properties are reported:

- Band structures.
- Electronic densities; partial (PDOS) and total (DOS).
- Density of states.

The main goal is to know the nature of the bonds between atoms.

II.5.1. Band structure

Figures II.5 and II.6 reflect the energies of the band structures calculated at points of high symmetries in the Brouillon zone (BZ) by TB-mBJ.

There are two zones: the conduction band (BC) which corresponds to positive energies, and the valence band (BV) corresponding to negative energies. The latter consists of an inner layer (low energies far from the Fermi level) and an outer layer (near the Fermi level).

The following outcomes are to be illustrated:

- Without TB-mBJ, an **indirect** gap of **0.28 eV** is attributed for our compound **Ag_2BaS_4Sn** at the points Γ-Z (figure II.5). The VB maximum is at the point Z and the CB minimum is at the point Γ.
- TB-mBJ undergoes an **indirect** gap of **1.37 eV** at the same points (figure II.6).

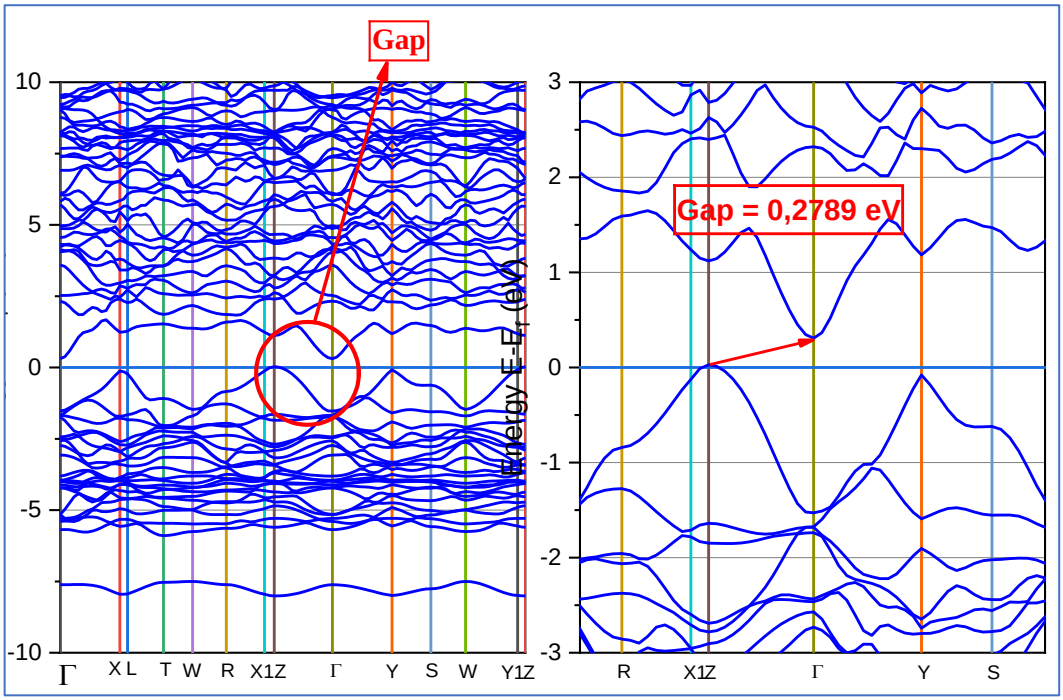

Figure II.5: Calculated band structure of Ag_2BaS_4Sn (without TB-mBJ).

The calculated band structure results are summarized in table II.6, where a comparison with experimental and/or theoretical results is provided.

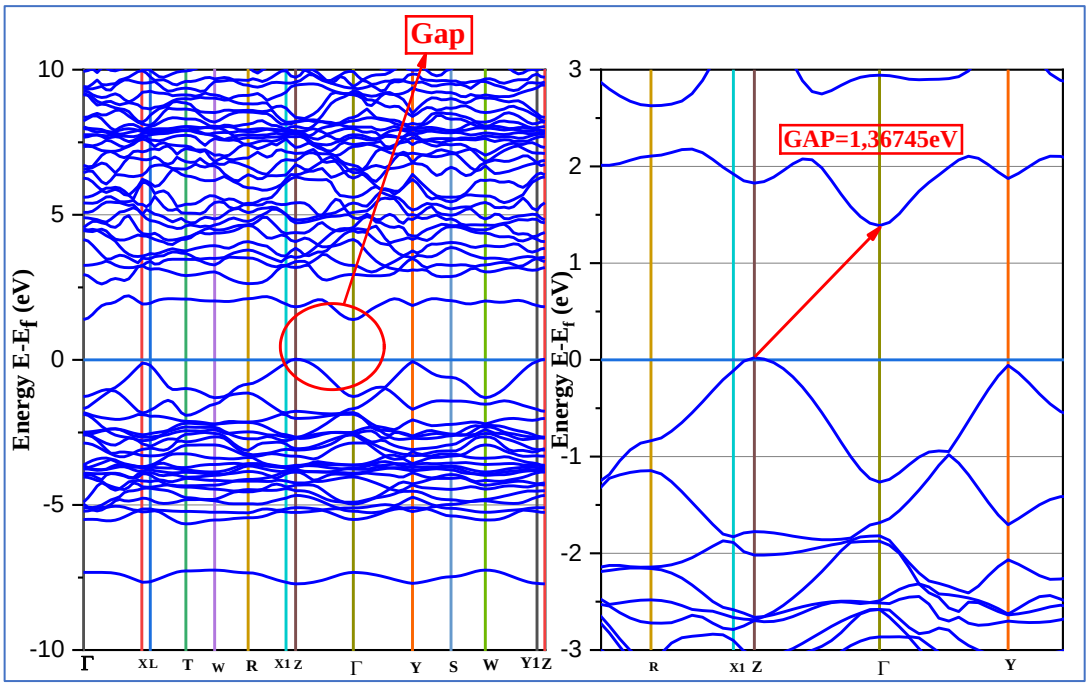

Figure II.6: Band structure calculated for Ag_2BaSnS_4 (with TB-mBJ).

Tableau II.6: Results relating to the band structure of Ag_2BaS_4Sn.

Compound	Method WC-GGA	Energy gap (eV)			
		Nature	Value	Exp.	Deviation (%)
Ag_2BaS_4Sn	Without TB-mBJ	I at Γ-Z	0.28	1.77 [9]	-84.18
	With TB-mBJ	I at Γ-Z	1.37		**-22.60**
	Théorie [9]	I	0.48		-72.88

D : direct. Sign (-) : under estimation.
I : indirect. Sign (+) : overestimation.

It is well known that the TB-mBJ gives a better estimation of the band gap energies (gap) of solids as is the case for the GW method and the hybrid HSE functional (implemented in the CASTEP code) but with a lower cost [12-15].

Thus, our result of 1.34 eV with TB-mBJ is closed compared to the experimental value of 1.77 eV (with -22.6% as deviation). Also, our value is more accurate than that of 0.48 eV reported from another theoretical study in reference [9] (with -72.88 eV as deviation) where authors did not adopt the HSE implemented in CASTEP code.

Our obtained results are slightly less than those reported for commercialized NLO chalcopyrite materials: $AgGaQ_2$ (Q = S, Se) and $ZnGeP_2$ [9, 16], which guaranties to our material a larger transparency range and a better damage threshold (DTS) compared with

the above mentioned chalcopyrites. This is due to the existence of correlation between gap value and optical DTS [16].

II.5.2. Density of states

The optical behaviors of materials are closely linked to electronic transitions from valence bands (BV) to conduction bands (BC), we then present densities of states (DOS) to identify the characteristics (structures) of electronic states.

We show in figures II.7 and II.8 the calculated total (TDOS) and partial (PDOS) state densities of the studied selenide. The Fermi level stands at 0eV.

As illustrated in these figures, we observe similarities in the shape of the densities with slight differences in the positions of the states as well as in their intensities.

Generally, the bands are narrow and relatively intense in the inner layer of the BV but moderately intense and broad near the fermi level. In BC, the bands are wider and relatively weak in intensity.

A deeper analysis of the densities of states reveals the following remarks:

The PDOSs were achieved and we find out that in the VB region below the Fermi level, the Ag-4d and S-3p states dominating the VB-1 region are mixing with minor Sn-5s and Sn-5p states. Above the Fermi level, the CB-1 region is derived primarily from the S-3p and Sn-5s states mixing with small amounts of Ag-4d and Sn-5p states.

The Ba atoms almost make no contribution around E_F and act as electron donors to stabilize the structure. Therefore, the band gap absorptions are primarily ascribed to the charge transitions from the S-3p states to Ag-4d, Sn-5s, and Sn-5p states.

II.5.3. Charge densities

The electronic charge density shows us the nature of the bonds in compounds, whether they are ionic, covalent or even mixed in nature.

The calculation of the charge densities leads into the results interpreted in figure II.9. Each projection translates the contours of the charge density on a plane containing the four atoms Ag, Ba, Sn, and S.

For charge density of Ag_2BaS_4Sn, the following remarks are noted:

- Around atoms Sn and S, the contours are well deformed, indicating thus a covalent Sn-S bond character. This correlates with the charge transitions from the S-3p states to Sn-5s and Sn-5p states (from DOS results).

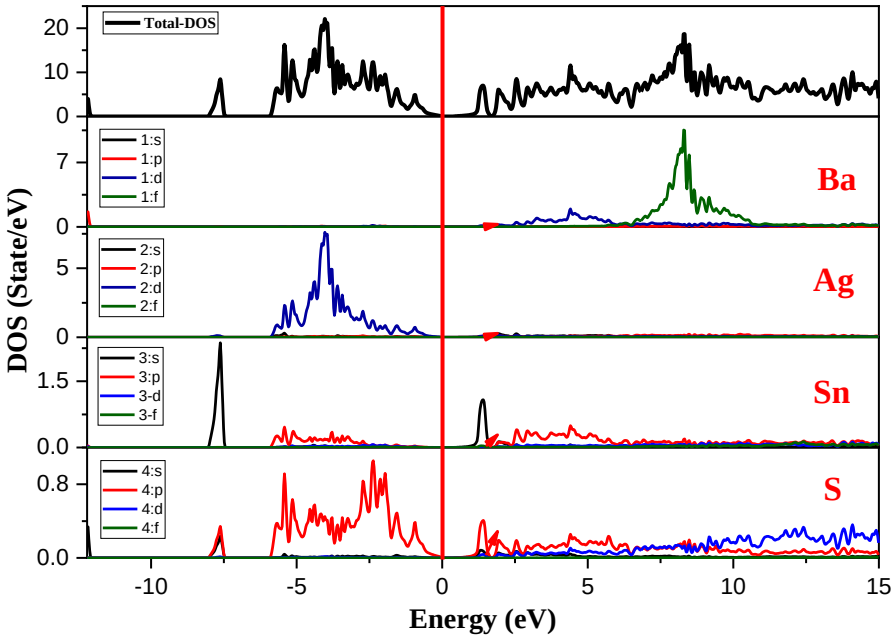

Figure II.7: Total and partial density of states calculated for Ag_2BaSnS_4.without TB-mBJ.

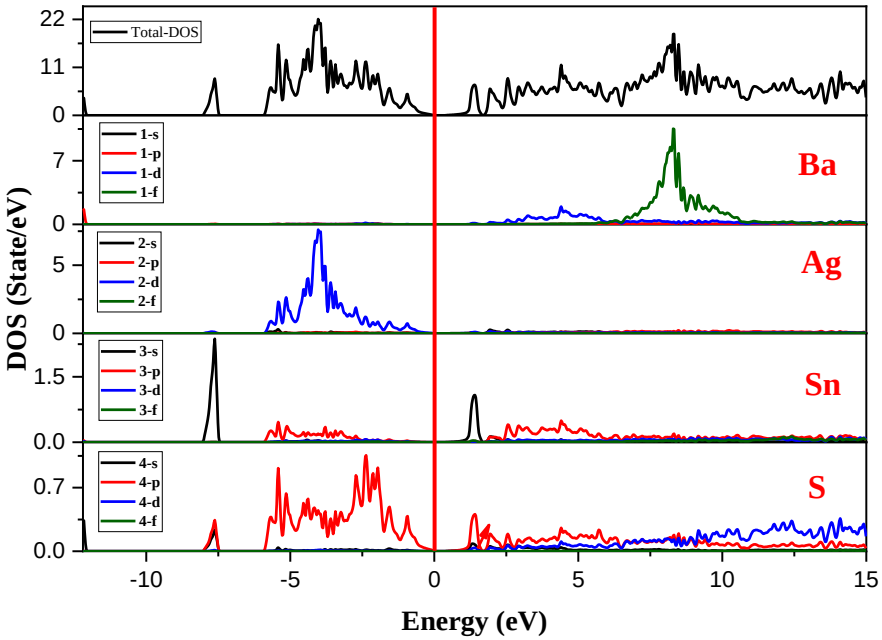

Figure II.8: Total and partial density of states calculated for Ag_2BaSnS_4.with TB-mBJ.

- For Ag and S atoms, the contours are also deformed, thus Ag-S bond is mainly covalent (charge transitions from the S-3p to Ag-4d states; from DOS results).
- The symmetry is almost spherical around the Ba and S atoms with a very slight deviation towards each other which indicates that the Ba-S bond is mainly ionic with a very weak covalent tendency. This result is a confirmation to the DOS results indicating the electron donor behavior of the Ba atom in order to stabilize the structure.

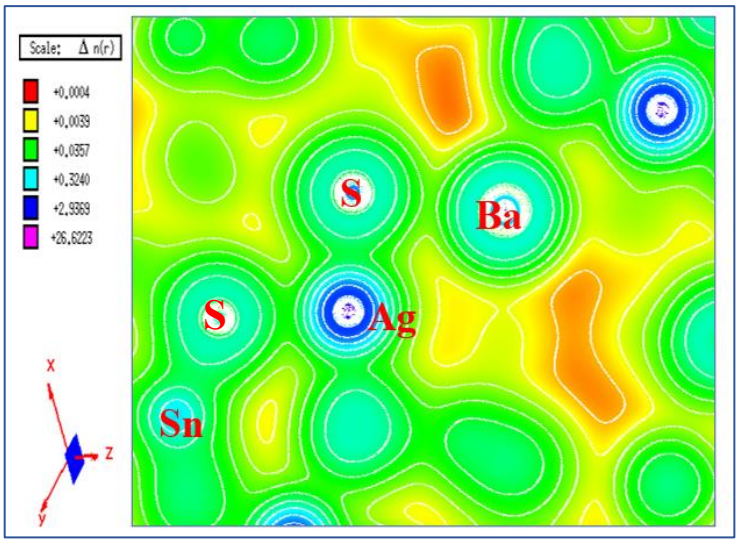

Figure II.9: Calculated charge density calculated in a plane containing Ag, Ba, Sn, and S atoms.

II.5.4. Liner optical properties

II.5.4.1. Dielectric function

The dielectric constant ε(ω) is the keystone for the exploitation and interpretation of the linear optical properties of materials. It is a complex function with a real part $\varepsilon_1(\omega)$ and an imaginary part $\varepsilon_2(\omega)$.

The imaginary part of the dielectric function is calculated from the probabilities of electronic transitions between valence band and conduction band. Its formula is given by the following equation [17]:

$$\varepsilon_2(\omega)=(Ve^2/2\hbar\pi m^2\omega^2)\sum_{n,\,n'}\int d_3k|<\mathbf{kn}|\mathbf{p}|\mathbf{kn}'>|^2 \quad X\, f(Kn)\big(1-f(Kn')\big)\delta(E_{Kn}-E_{Kn}-\hbar\omega) \qquad \text{II.1}$$

With:

- V: cell volume.
- e: electron charge.
- m: electron mass.
- ħω: energy of the incident photon.
- f(kn): Fermi-Dirac distribution.
- p: angular momentum operator.
- kn: wave function.

For the real part, the calculation is done using the following relation [18-20]:

$$\varepsilon_1(\omega) = 1 + \left(\frac{2}{\pi}\right)\int_0^{\infty}\{[\varepsilon_2(\omega).\omega'.\mathrm{d}\omega']/[\omega'^2-\omega^2]\} \qquad \text{II.2}$$

The calculations carried out on the dielectric functions (real parts $\varepsilon_1(\omega)$ and imaginary parts $\varepsilon_2(\omega)$) led to the results illustrated in figures II.10 and II.11.

The peaks in the imaginary part of the dielectric function correspond to electronic transitions between valence bands and conduction bands.

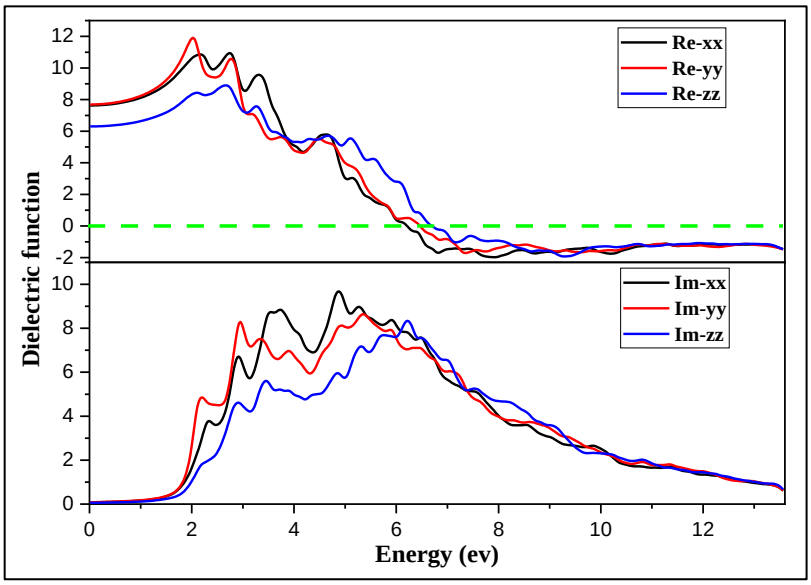

Figure II.10: Calculated imaginary $\varepsilon_2(\omega)$ and real $\varepsilon_1(\omega)$ parts of the dielectric function of Ag_2BaS_4Sn without TB-mBJ.

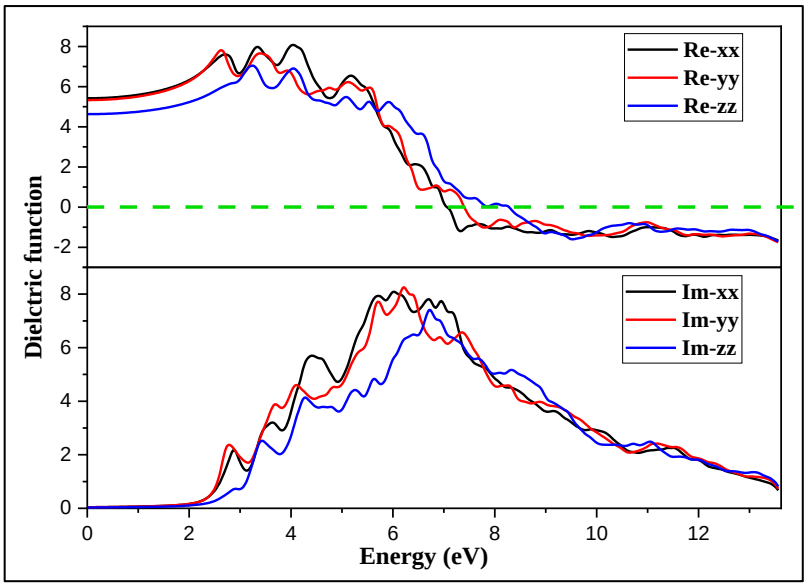

Figure II.11: Calculated imaginary $\varepsilon_2(\omega)$ and real $\varepsilon_1(\omega)$ parts of the dielectric function of Ag_2BaS_4Sn with TB-mBJ.

According to the results obtained, our material presents major peaks corresponding to electronic transitions from **S-3p** (BV) toward **Sn-5p,5s** (BC). Transitions from **S-3p** (BV) toward **Ag-4d** (BC) also participate.

II.5.4.2. Static refraction indices

The static refractive indices are calculated from the real part of the dielectric function at $\varepsilon_1(0)$, this is its most important quantity. Table II.7 presents their values.

Tableau II.7: Static refractive indices calculated for Ag_2BaS_4Sn.

Ag_2BaS_4Sn	n_x	n_y	n_z
Without TB-mBJ	2.762	2.773	2.610
With TB-mBJ	2.328	2.308	2.151

II.5.4.3. Other linear optical properties

All other properties can be calculated from both the real and imaginary parts of the dielectric function:

- Absorption **I(ω)**: to estimate the optical gap.
- Reflectivity **R(ω)**.
- Energy loss **L(ω)**: describes the energy of an accelerated electron passing through the crystal.
- Refractive index **n(ω)**.

The equations II.4 to II.7 below allow the calculation of these properties.

$$I(\omega) = \sqrt{2\omega}.\left[\sqrt{\varepsilon_1^2(\omega) + \varepsilon_2^2(\omega)} - \varepsilon_1(\omega)^{1/2}\right] \quad \text{II.4}$$

$$R(\omega) = \left[(\sqrt{\varepsilon(\omega)} - 1)/(\sqrt{\varepsilon(\omega)} + 1)\right]^2 \quad \text{II.5}$$

$$L(\omega) = \varepsilon_2(\omega)/(\varepsilon_1^2(\omega) + \varepsilon_2^2(\omega)) \quad \text{II.6}$$

$$n(\omega) = 1/\sqrt{2}\left[\sqrt{\varepsilon_1^2(\omega) + \varepsilon_2^2(\omega)} + \varepsilon_1(\omega)\right]^{1/2} \quad \text{II.7}$$

The calculation results obtained for these four parameters are illustrated in figures II.12 and II.13.

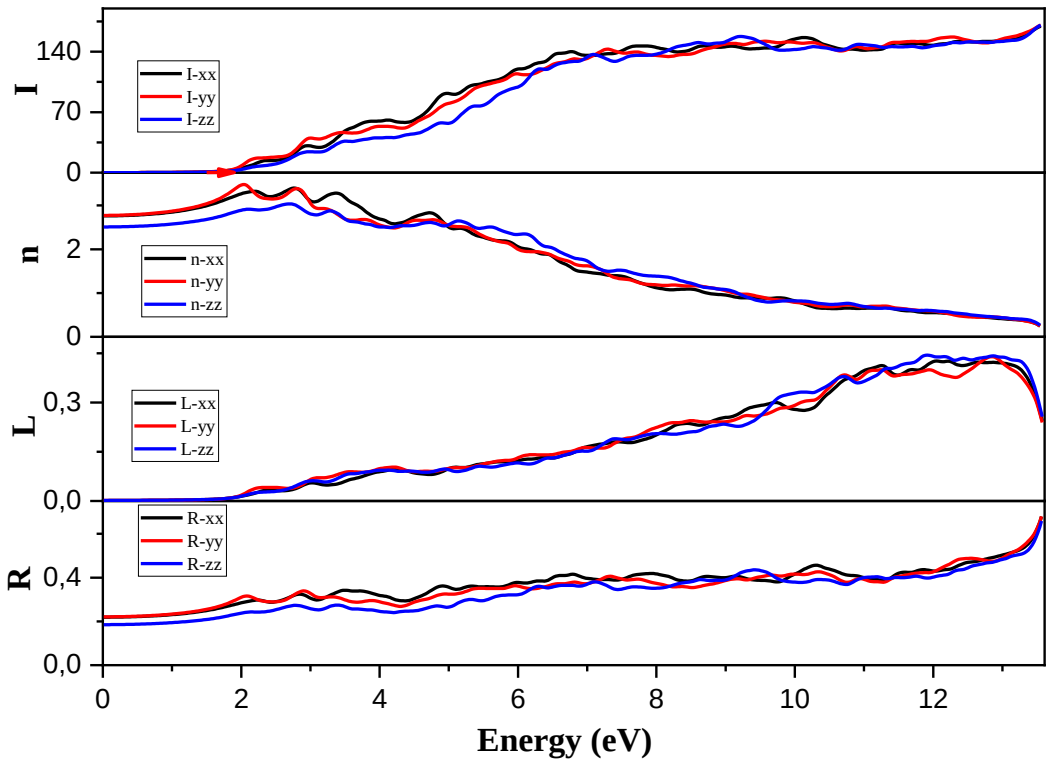

Figure II.12: Calculated optical properties for Ag_2BaS_4Sn as function of the incident photon energy (eV): absorption coefficient **I** (10^4/cm), reflectivity **R**, energy loss **L**, and refraction index **n** (without TB-mBJ).

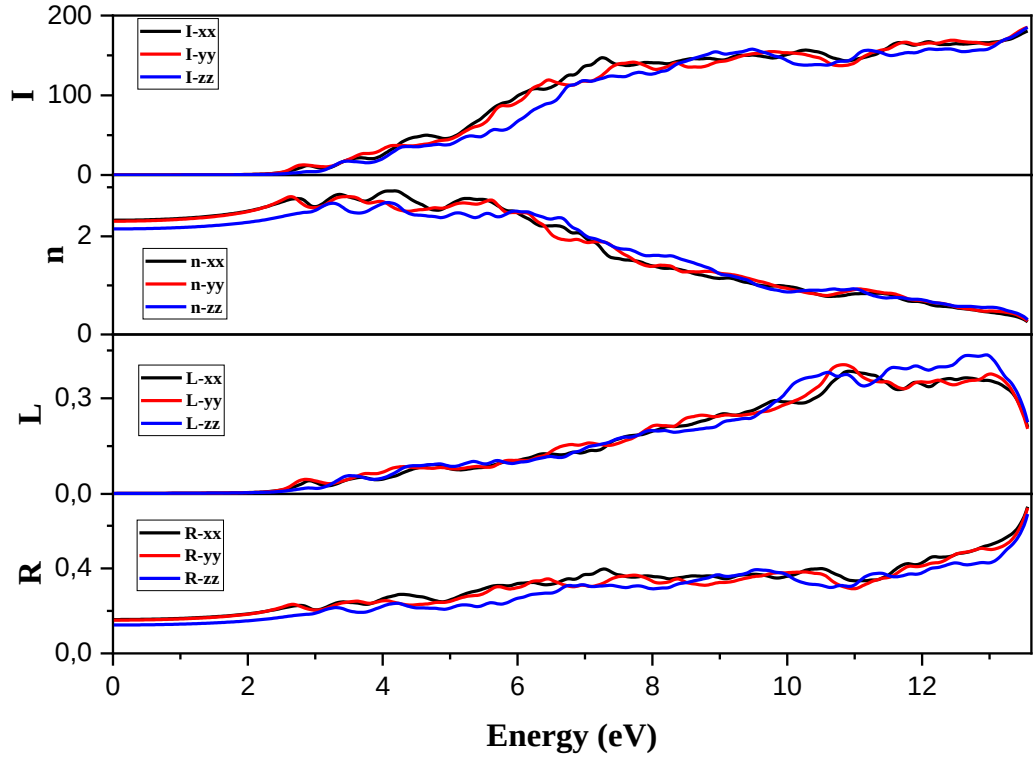

Figure II.13: Calculated optical properties for Ag_2BaS_4Sn as function of the incident photon energy (eV): absorption coefficient **I** (10^4/cm), reflectivity **R**, energy loss **L**, and refraction index **n** (with TB-mBJ).

In the energy loss **L(ω)** diagramm, the most important pic corresponds to the plasma frequency ω_p where we notice a sharp reduction in reflectivity **R(ω).** Values of energies corresponding to those caracteristic pics are grouped in table II.8.

Tableau II.8: Loss of energy **L(ω)** of Ag_2BaS_4Sn (10^4/cm).

Ag_2BaS_4Sn	Energy loss L(ω) at ω_p (10^4/cm)		
	$L(\omega_\rho)_{XX}$(eV)	$L(\omega_\rho)_{yy}$(eV)	$L(\omega_\rho)_{ZZ}$(eV)
Without TB-mBJ	0.426 (12.04)	0.439 (12.83)	0.444 (11.90)
With TB-mBJ	0.385 (10.92)	0.405 (10.82)	0.436 (12.94)

From the absorption spectra I(ω) we can derive the values of the optical gaps of our material. The values for Ag_2BaS_4Sn are represented in table II.9.

Tableau II.9: Optical gap values (energy at I_0) for Ag_2BaS_4Sn.

Ag_2BaS_4Sn	Energy at I_0 ≡ Optical gap (eV)		
	$E[I(0)_{XX}]$	$E[I(0)_{yy}]$	$E[I(0)_{ZZ}]$
Without TB-mBJ	0.80	0.78	0.94
With TB-mBJ	1.24	1.21	1.40

Optical gap values are close to electronic ones indicating the reliability of our calculations.

The birefringence (n_0-n_e) informs us about the nature of the material (uniaxial or biaxial, positive or negative).

The birefringence is illustrated in figures II.14 and II.15 and its static limit values and its maximum values with their corresponding energies are indicated in table II.10.

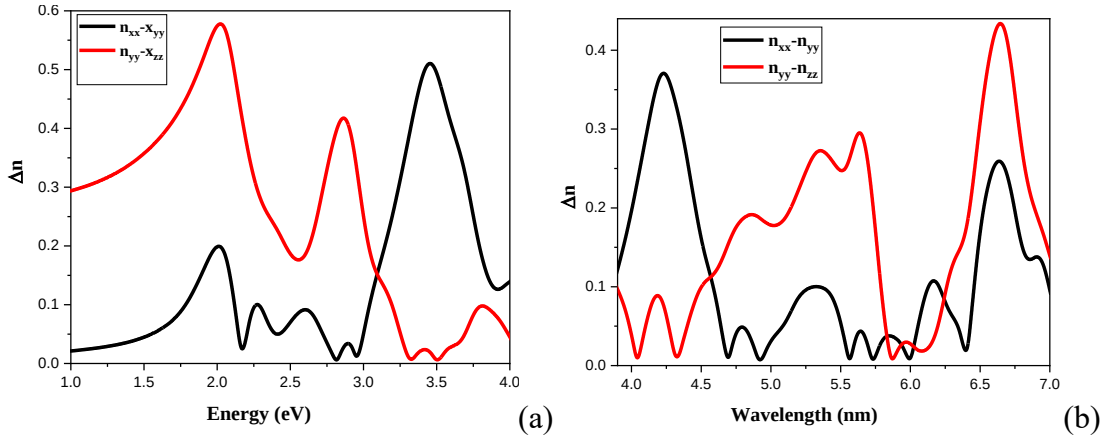

Figure II.14: Calculated birefringence Δn for Ag_2BaS_4Sn with (b) and without (a) TB-mBJ.

Table II.10: Values of the birefringence (Δn) of the compound Ag_2BaS_4Sn.

Ag_2BaS_4Sn	Birefringence (Δn)			
	At the static limit		Maximum value (energy in eV)	
	xx-yy	yy-zz	xx-yy	yy-zz
Without TB-mBJ	0.011	0.263	0.511 (3.44)	0.580 (2.03)
With TB-mBJ	0.019	0.157	0.372 (4.23)	0.436 (6.65)

Concerning the maximum value of birefringence for our material, it can be noted from the reported values (table II.10) that the large values are located at lower energies while the less important values are located at lower energies. This means that the more the max value of birefringence increases the more it will be at a lower energy.

In addition, we extract birefringence values at 2050 nm (equivalent to 0.61 eV) and we find out the value of 0.089 compared to 0.052 calculated in reference [9].

II.6. Conclusion

From the reported results, we can conclude that our material is a semiconductor of choice with a more or less wide transparency window. Also, from the calculated properties, we found that TB-mBJ considerably improves the estimation of the electronic properties and especially that of the bandgap.

On the other hand, the choice of approximation turns out to be important because the results of the calculated properties change from one approximation to another.

References

[1]: P. Blaha; K. Schwarz; G.K.H. Madsen; D. Kvasnicka; J. Luitz; R. Laskowski; F. Tran; L.D. Marks. **WIEN2K An augmented plane wave plus local orbitals program for calculating crystal properties.** Vienna University of Technology. Austria (2018).

[2]: J.C. Slater. Phys. Rev. 51 (1937) 846.

[3]: K.P. Perdew, K. Burke, M. Ernzerhof. **Phys. Rev. Lett.** 77(18) (1996) 3865.

[4]: K. Schwarz, P. Blaha, G.K.H. Madsen. **Computer Physics Communications** 147 (2002) 71.

[5]: S. Baroni, S. de Gironcoli, A. Dal Corso, P. Giannozzi. **Rev. Mod. Phys.** 73 (2001) 515.

[6]: H.B. Schlegel. **J. Comp. Chem.** 3 (1982) 214.

[7]: F. Tran, P. Blaha. **Phys. Rev. Lett.** 102 (2009) 226401.

[8]: K. Momma, F. Izumi. **J. Appl. Cryst.** 44 (2011) 1272: VESTA (Vizualization for Electronic and Structural Analysis) Ver. 3.4.2. (2017).

[9]: H. Chen, P-F. Liu, B-X. Li, H. Lin, L-M. Wu, X-T. Wu. **Dalton Trans.** 47 (2018) 429.

[10]: L. Nian, K. Wu, G. He, Z. Yang, S. Pan. **Inorg. Chem.**

[11]: B. Lagoun, B. Bentria, I.K. Lefkaier. **Physica B** 433 (2014) 117.

[12]: J.P. Perdew, A. Ruzsinszky, G.I. Csonka, O.A. Vydrov, G.E. Scuseria, L.A. Constantin, X. Zhou, K. Burke. **Phys. Rev. Lett.** 102 (2009) 039902.

[13]: R. Abt, C. Ambrosch-Draxl, P. Knoll. **Physica B** 194 (1994) 1451.

[14]: C. Ambrosch-Draxl, J. O. Sofo. **Comput. Phys. Commun.** 175 (2006) 1.

[15]: D. J. Singh. **Phys. Rev.** B 82 (2010) 205102.

[16]: O. Madelung. **Semiconductors: Data Handbook**. 3rd ed. Springer. Berlin (2004).

[17]: S. Saha, T.P. Sinha. **Phys. Rev.** B 62(13) (2000) 8828.

[18]: H.A. Kramers. **Nature** 113(2845) (1924) 673.

[19]: H.A. Kramers. **Nature** 114(2845) (1924) 310.

[20]: R. DE L. Kronig. **J. Opt. Soc. America** 12(6) (1926) 547.

General conclusion

In this work, we have studied the structural, electronic (band structure, density of states), and optical (dielectric function, absorption coefficient, reflectivity, energy loss, refractive index) properties of the compound Ag_2BaSnS_4 by the method of linearized augmented plane wave at full potential (FP-LAPW) in the framework of DFT, it is treated with the approximation of the generalized gradient approximation (GGA), implemented in the code WIEN2K.

In this conclusion, we would like to emphasize the following essential points: first of all, we studied the structural properties which characterize the ground state of the system considered such as the equilibrium volume. Our results are in very good agreement with experimental results.

Next, we determined the electronic properties which indicate that our compound has indirect gap.

The DOS allowed us to examine the different coordination modes of Ag_2BaSnS_4, we obtained the nature of the bond Sn-S (covalent) and for Ag-S is mainly covalent , while Ba-S bond is mainly ionic.

To study the behavior of our semiconductor compound with respect to light, we calculated its optical properties such as the dielectric function, reflectivity, absorption coefficient, refractive index, etc.

Finally, according to our short experiment on the use of the WIEN2K code it turns out that this program is a very powerful code which allows the prediction of most of the physical properties of materials.

عنوان المذكرة: نظرة ثاقبة على الخصائص الفيزيائية للمركب Ag_2BaSnS_4: دراسة DFT

الاسم و اللقب: بن عرفة محمد الطيب و حياني رياض **المؤطر: د. صوراية بلحاج**

ملخص: لقد أجرينا حسابات أولية عن الخواص التركيبية والإلكترونية لمركب Ag_2BaSe_4Si الهدف من هذه الدراسة هو تحديد فجوة هذا أشباه الموصلات، وهو مثير للاهتمام في التطبيقات الإلكترونية البصرية. تم إجراء الحساب باستخدام الطريقة الخطية لإجمالي الموجات المستوية المعززة المحتملة (FP-LAPW) المطبقة في كود Wien2k، في إطار نظرية الكثافة الوظيفية (DFT) باستخدام تقريب (WC-GGA) واستخدام إمكانات Becke-Johnson المعدلة (TB-mBJ)
النتائج التي تم الحصول عليها تتفق مع النتائج التجريبية. تم حساب بنية النطاق الإلكتروني والكثافة الجزئية والكلية للحالات.

كلمات مفتاحية: الحسابات الأولية ، FP-LAPW، DFT، WC-GGA، البنية الإلكترونية، فجوة النطاق، كثافة الحالات، أشباه الموصلات II-VI.

Memory title: Insight into the physical properties of the compound Ag_2BaSnS_4: DFT study.

First and last name : BENARFA Mohamed Tayeb HAYANI Riyad **Directed by: Dr. Soraya BELHADJ**

Abstract: We had performed ab- initio calculations structural and electronic properties of $Ag_2BaSeSi_4$ compound. The objective of this study is to determine the gap of this semiconductor, it is interesting in optoelectronic applications. The calculation was carried out using the linear method of total potential augmented plane waves (FP-LAPW) implemented in the Wien2k code, within the framework of density functional theory (DFT) using the approximation of WC-GGA and using the modified Becke-Johnson potential (TB-mBJ).
The results obtained are in agreement with the experimental results. The electronic band structure and partial and total densities of states were also calculated.

Key words: ab- initio calculations, FP-LAPW, DFT, WC- GGA, electronic structure, bandgap, density of states, II-VI semiconductors.

Titre du mémoire: Aperçu des propriétés physiques du composé Ag_2BaSnS_4 : étude DFT.

Nom et prénom: BENARFA mohamed tayeb et HAYANI Riyad **Encadreur: Dr. Soraya BELHADJ**

Résumé: Nous avons effectué des calculs ab-initio des propriétés structurales et électroniques de composé Ag2BaSeSi4. L'objectif de cette étude est de déterminer le gap de ce semi-conducteur, il est intéressant dans les applications optoélectroniques. Le calcul a été effectué en utilisant la méthode linéaire des ondes planes augmentées à potentiel total (FP-LAPW) implanté dans le code Wien2k, dans le cadre de la théorie de la fonctionnelle de densité (DFT) en utilisant l'approximation de la WC-GGA en utilisant le potentiel modifié de Becke-Johnson (TB-mBJ) .
Les résultats obtenus sont en concordance avec les résultats expérimentaux. La structure de bande électronique et les densités d'états partielles et totales ont été calculées.

Mots clés: Calculs ab-initio, FP-LAPW, DFT, WC-GGA, structure électronique, bande interdite, densité d'états, semi-conducteurs II-VI.